Prediction of early summer rainfall over South China by a physical-empirical model

So-Young Yim, Bin Wang & Wen Xing

Climate Dynamics
Observational, Theoretical and Computational Research on the Climate System

ISSN 0930-7575

Clim Dyn
DOI 10.1007/s00382-013-2014-3

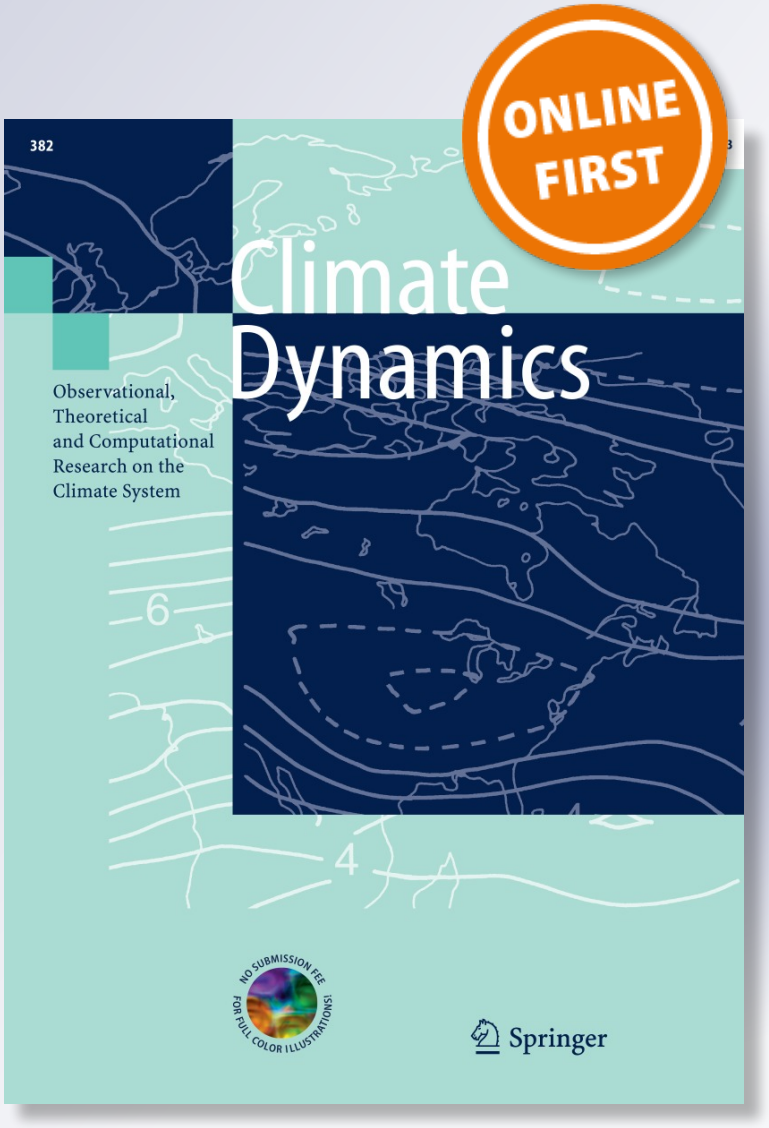

Springer

Clim Dyn
DOI 10.1007/s00382-013-2014-3

Prediction of early summer rainfall over South China by a physical-empirical model

So-Young Yim · Bin Wang · Wen Xing

Received: 31 August 2013 / Accepted: 28 November 2013

Abstract In early summer (May–June, MJ) the strongest rainfall belt of the northern hemisphere occurs over the East Asian (EA) subtropical front. During this period the South China (SC) rainfall reaches its annual peak and represents the maximum rainfall variability over EA. Hence we establish an SC rainfall index, which is the MJ mean precipitation averaged over 72 stations over SC (south of 28°N and east of 110°E) and represents superbly the leading empirical orthogonal function mode of MJ precipitation variability over EA. In order to predict SC rainfall, we established a physical-empirical model. Analysis of 34-year observations (1979–2012) reveals three physically consequential predictors. A plentiful SC rainfall is preceded in the previous winter by (a) a dipole sea surface temperature (SST) tendency in the Indo-Pacific warm pool, (b) a tripolar SST tendency in North Atlantic Ocean, and (c) a warming tendency in northern Asia. These precursors foreshadow enhanced Philippine Sea subtropical High and Okhotsk High in early summer, which are controlling factors for enhanced subtropical frontal rainfall. The physical empirical model built on these predictors achieves a cross-validated forecast correlation skill of 0.75 for 1979–2012. Surprisingly, this skill is substantially higher than four-dynamical models' ensemble prediction for 1979–2010 period (0.15). The results here suggest that the low prediction skill of current dynamical models is largely due to models' deficiency and the dynamical prediction has large room to improve.

Keywords South China rainfall index (SCRI) · East Asian subtropical front · Indo-Pacific warm pool SST · North Atlantic Ocean · Philippine Sea subtropical High · Okhotsk High · Physical-empirical model

1 Introduction

South China (SC) is referred to a region south of the Yangtze River and east of the Tibetan Plateau, or mainly south of 28°N and east of 110°E. This is a major foodgrain production region of China. Prediction of summer monsoon rainfall is critical to agriculture planning and water resources management. Yet, its seasonal prediction has been a long standing challenge for the operational forecasting community.

One of the difficulties for East Asian summer monsoon (EASM) prediction is linked to prominent seasonal migration of the subtropical monsoon rain band from May to August (Tao and Chen 1987). Traditionally, the prediction of EASM deals with June–July–August (JJA) mean anomalies. Wang et al. (2009a) and Qin et al. (2013) have shown that the May and June rainfall patterns are similar; likewise the July and August rainfall patterns are also similar. However, there are remarkable differences in the mean states between early summer (May–June, "MJ") and late summer (July–August, "JA"); further, the principal modes of interannual precipitation variability also exhibit distinct spatial and temporal structures during the early and late summer. They concluded that the EASM prediction may be beneficial if making MJ and JA summer prediction, separately.

S.-Y. Yim (✉) · B. Wang · W. Xing
International Pacific Research Center, University of Hawaii at Manoa, Honolulu, HI 96822, USA
e-mail: hiyim03@gmail.com

B. Wang
Department of Meteorology, University of Hawaii at Manoa, Honolulu, HI 96822, USA

Published online: 11 December 2013

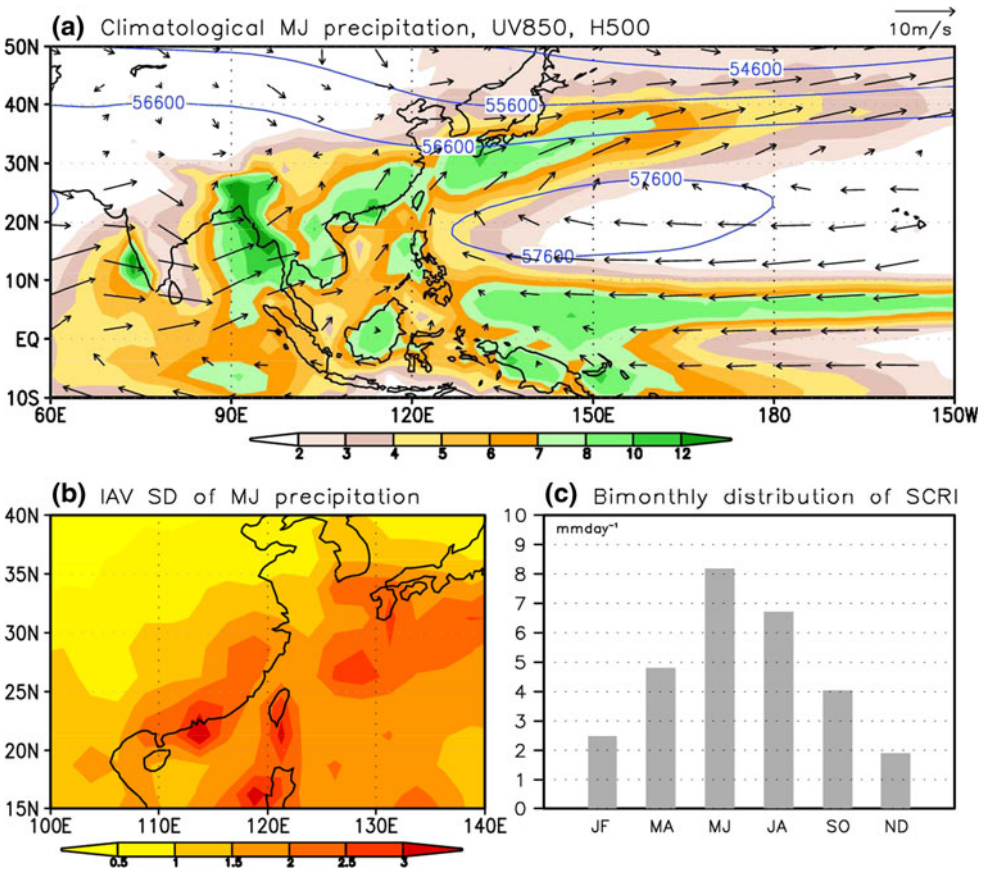

Fig. 1 **a** Climatological MJ (May–June) mean precipitation (mm/day), 850-hPa winds (UV850) (m/s) and 500 hPa geopotential height (H500) (m^2/s^2). **b** Interannual variability (IAV) standard deviation (SD) of MJ precipitation. **c** Bi-monthly distribution of South China rainfall index (SCRI) from January to December. The GPCP V2 data were used for the period 1979–2012

Different from traditional JJA forecast, this study focuses on MJ rainfall prediction. This period involves the onset of South China Sea monsoon in mid-May and the Meiyu onset over China and Baiu onset in South Japan in early and mid-June. The MJ EASM is characterized by a prominent rainfall band from Bay of Bengal extending northeastward to south of Japan in the WNP (Fig. 1a), which is a salient feature of the global precipitation in MJ. Note that SC is a center of the MJ mean precipitation (near Hong Kong, Fig. 1a) and also exhibits the largest interannual variability (Fig. 1b). Locally, MJ is the peak rainy season over the SC (Fig. 1c). For all these reasons, the present study will focus on SC rainfall prediction in MJ.

In spite of the fact that the state-of-the art climate prediction models have been improved steadily over the past two decades, the current coupled climate models have rather limited skills in seasonal prediction of EASM precipitation in general (Wang et al. 2009b). The areal averaged hindcast skill for summer (June–July–August) rainfall over East Asia (EA) (5°N–45°N, 100°E−140°E) is only about 0.21 in terms of temporal correlation (Wang et al. 2013).

Our study aims to identify the physical precursors to predict SC rainfall 2-month ahead and to examine their physical linkages with the MJ SC rainfall variability. We also predict the SC rainfall by establishing physically based-empirical prediction model. The physical-empirical model can help us understand that the dynamic models' low prediction skill is due to intrinsic limit on predictability or due to models' deficiency. The data and method used are described in Sect. 2. The climate anomalies associated with MJ SC rainfall index and physical predictors are presented in Sect. 3. The result of a physical-empirical model of MJ SC rainfall is described in Sect. 4. Section 5 provides our conclusion and discussion.

2 Data and method

The precipitation data used in our study are derived from 72 meteorological stations that are well distributed in SC for the period 1979–2010 provided by Chinese Meteorological Information Center. For comparison, Global Precipitation Climatology Project (GPCP) version 2.2 (Huffman et al. 2011) data are also used, which have been shown to be reliable in revealing long-term variability (Zhou et al. 2008; Wang et al. 2012). The atmospheric circulation and sea surface temperature (SST) data were obtained from the newly released ERA interim (Dee et al. 2011) and the National Oceanic and Atmospheric Administration extended reconstructed SST (ERSST) version 3

(Smith et al. 2008), respectively. Our study focuses on the period of 1979–2012, because there was a prominent decadal shift in the late 1970s, which have caused significant changes in the EASM-El Nino-Southern Oscillation (ENSO) relationship (Wu and Wang 2002; Zhou et al. 2009; Yun et al. 2010). Focusing on the recent 34 years can partially avoid the complexity arising from multi-decadal impacts on the year-to-year variations.

This study used four state-of-the-art atmosphere-ocean-land coupled models including NCEP CFS version 2 (Saha et al. 2013), ABOM POAMA version 2.4 (Hudson et al. 2011), GFDL CM version 2.1 (Delworth et al. 2006), and FRCGC SINTEX-F model (Luo et al. 2005), which were adopted from Asia-Pacific economic cooperation climate center (APCC)/climate prediction and its application to society (CliPAS). The hindcast datasets we used are detailed by Wang et al. (2009b). To compare with the empirical forecast, retrospective forecasts with March 1st initial condition were used for the available period of 1979–2010 targeting 2-month lead MJ seasonal prediction. The multi-model ensemble (MME) prediction was made by simply averaging of the four coupled models' ensemble mean anomalies after removing their own climatology.

Stepwise regression was used to establish the physical-empirical model. Prior to regression, all variables are normalized by removing their means and divided by their corresponding standard deviation, which allows direct comparison of the relative contribution of each predictor by examining the normalized regression coefficient. The stepwise procedure identifies important predictors at each step. The significance of each predictor selected is based on significance in increase of the regressed variance by a standard F test (Panofsky and Brier 1968). A 95 % statistical significance level is required for an individual variable to be included in the predictor pool. Once enter in the model, a predictor can only be removed if its significance level falls below 95 % by the addition/removal of another variable. To avoid over-fitting, we require the number of selected predictors is less than 10 % of the sample size.

3 Interannual variation of the South China precipitation

3.1 A convenient measure of the early summer rainfall variability over South China and East Asian subtropical front

To facilitate study the interannual variation of the SC MJ rainfall, we construct a SC rainfall index (SCRI) that represents the MJ mean precipitation rate averaged over the 72 stations over SC as shown in Fig. 2. The physical consideration for establishing such an index is based on a major mode analysis. The leading empirical orthogonal function (EOF1) mode of the MJ precipitation over the EA region (15°N–40°N, 100°E−140°E) has a maximum loading at the SC (Fig. 2a), suggesting that the variability within SC region is largely coherent and the SC is the center of action for MJ rainfall variability over EA. The MJ SCRI is highly correlated with the leading EOF principal component (PC1) with a temporal correlation coefficient (TCC) of 0.88 (Fig. 2b). Thus, the MJ SCRI represents faithfully the leading EOF mode of MJ precipitation variability over EA. We also compared the SCRI with the area-weighted mean MJ precipitation rate averaged over a rectangular region (21.25°N–28.75°N, 110°E−120°E) that derived from GPCP v2.2 dataset (Fig. 2a). The precipitation variability averaged over the rectangular region by GPCP data are in an excellent agreement with the MJ SCRI defined by using the station data and their correlation coefficient is 0.93 (1979–2010).

3.2 Large scale anomalies associated with a strong SCRI

Before searching predictors, we examine the simultaneous large-scale anomalies associated with a positive SCRI (Fig. 3). First, a positive SCRI represents an enhancement of the entire Meiyu/Baiu frontal rainfall, stretching from SC to south of Japan (Fig. 3a). There is an out-of-phase variation between the western North Pacific (WNP) and Meiyu/Baiu rainfall. The precipitation pattern tends to have a planetary zonal scale, which suggests that SC rainfall may have a good potential predictability due to its linkage with large scale subtropical front. In addition, on EA regional scale, a narrow, suppressed rainfall zone is seen just to the north of the enhanced Meiyu/Baiu band and further north a localized positive precipitation is found over the northern Korean peninsula. Second, in correspondence with the rainfall anomalies over the WNP, pronounced anticyclone anomaly is seen in the South China Sea and Philippine Sea, which enhances southwesterly winds along the northwest flank of the anticyclone and leads to increasing precipitation over the South China and Meiyu/Baiu by transporting abundant moisture toward the EA subtropical monsoon frontal zone (Fig. 3b). Third, the Okhotsk High pressure and associated anticyclonic winds are strengthened along with reduced precipitation. This confirms that the Okhotsk High is one of the crucial systems in characterizing the Meiyu/Baiu system (Ding 1992). The Okhotsk High brings cold air from north to meet with warm and moist subtropical southwesterlies, enhancing SC rainfall.

Associated with a positive SCRI are significant positive SST anomalies in the northern Indian Ocean, South China Sea and East of Taiwan (Fig. 3c), which is accompanied by

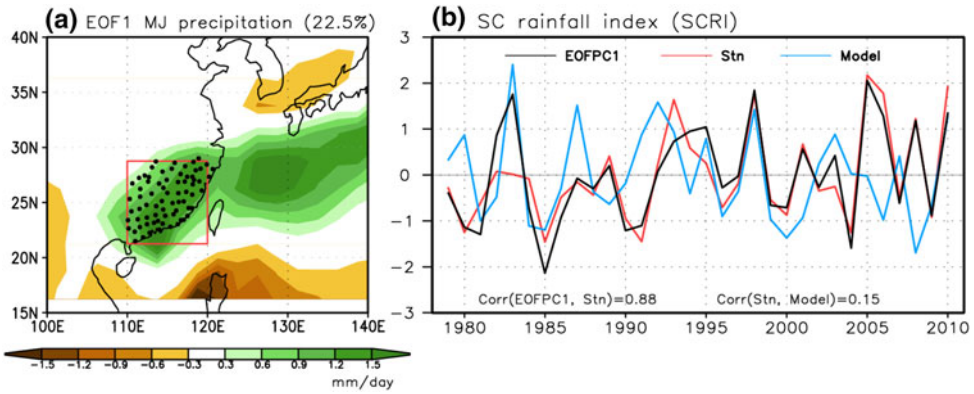

Fig. 2 The spatial pattern of leading mode (EOF1) of MJ precipitation over East Asia (**a**) and the normalized time series of corresponding principal component (*black*) (**b**). For comparison, the Southern China rainfall index (SCRI) derived from the 72 rain gauges stations data (*red*), and the multi-model retrospective prediction of the SCRI (*blue line*) are also plotted in (**b**). The *black dots* denote locations of the selected rain gauge stations (Stn) which were used to make an area averaged SCRI. The *red box* indicates the South China region when GPCP data are used to estimate the SCRI

slightly increased precipitation (or latent heating) over the northern Indian Ocean (Fig. 3a). On the other hand, to the eastern side of the anomalous Philippine Sea anticyclone are negative SST anomalies (albeit weak) and suppressed rainfall. This dipole SST anomaly pattern in the Indo-Pacific warm pool region implies a positive feedback between the anomalous Philippine Sea anticyclone and underlying ocean mixed layer that can maintain both the Philippine Sea anticyclone and the dipole SST anomalies (Wang et al. 2000, 2013). Another interesting feature is that a distinct north-south sea level pressure (SLP) contrasts occurring in North Atlantic, which is coupled with a tripolar SST anomalies (Fig. 3b, c).

In sum, the salient features associated with enhanced SC rainfall include (a) enhanced Philippine Sea anticyclone and associated dipolar SST anomalies over the Indo-Pacific warm pool, (b) the North Atlantic tripolar SST anomalies, and (c) enhanced Okhotsk High and associated warming air temperature anomalies. These features provide illuminating hints for searching for predictors.

3.3 Physical precursor signals in the previous winter

In order to predict SCRI 2-month ahead, we have examined climate anomalies in SST, 2 m air temperature and SLP in the preceding winter. Analysis of a large number of correlation maps reveals that the SST and 2 m air temperature *tendency* fields across winter season from December to February have the best indicative signals. Figure 4 shows the correlation maps of SST anomalies over ocean and 2 m air temperature (T2M) anomalies over land across winter from December to February associated with MJ SCRI. Three physically meaningful predictors are found.

First, a strengthened MJ SC rainfall is associated with a dipolar SST tendency over the Indian Ocean and WNP (IOWPTT), i.e., a warming tendency in eastern Indian Ocean and north of the Philippine Sea, and a negative SST anomaly southeast of the Philippine Sea. The warming to the northwest of Philippine Sea and the cooling to its southeast imply an enhancement of Philippine Sea high pressure (anticyclone) (Wang et al. 2000). Numerical experiments have shown that the positive thermodynamic feedback between the Philippine Sea anticyclonic anomaly and underlying SST dipole anomalies can maintain both the Philippine Sea anticyclone and the SST dipole through spring to early summer (Lau et al. 2005; Wang et al. 2013; Xiang and Wang 2013). It is a precursor for the enhanced MJ Philippine Sea anticyclone (Fig. 3b). The warming tendency over the Indian Ocean signifies development of the northern Indian Ocean warming and results in strong warming there in March and April (MA) (Fig. 5a) persisting into to early summer that increases in situ precipitation (Fig. 3a). The Indian Ocean warming-induced precipitation heating can also enhance the Philippine Sea anticyclone.

The second predictor is the tri-polar SST tendency across winter over North Atlantic (NATT). This tripolar tendency consists of a warming process in the tropical and mid-latitude North Atlantic and a cooling in the subtropics. This winter SST tendency establishes well-defined tripolar SST anomalies in March and April, which are coupled with a negative phase of North Atlantic Oscillation (NAO) (Fig. 5b). Due to a positive feedback between the atmosphere and ocean, the tripolar SST anomalies can sustain the negative phase of NAO or an Arctic Oscillation (AO) (Fig. 3b). It was proposed that the North Atlantic tripolar SST anomalies and NAO can influence Okhotsk High by

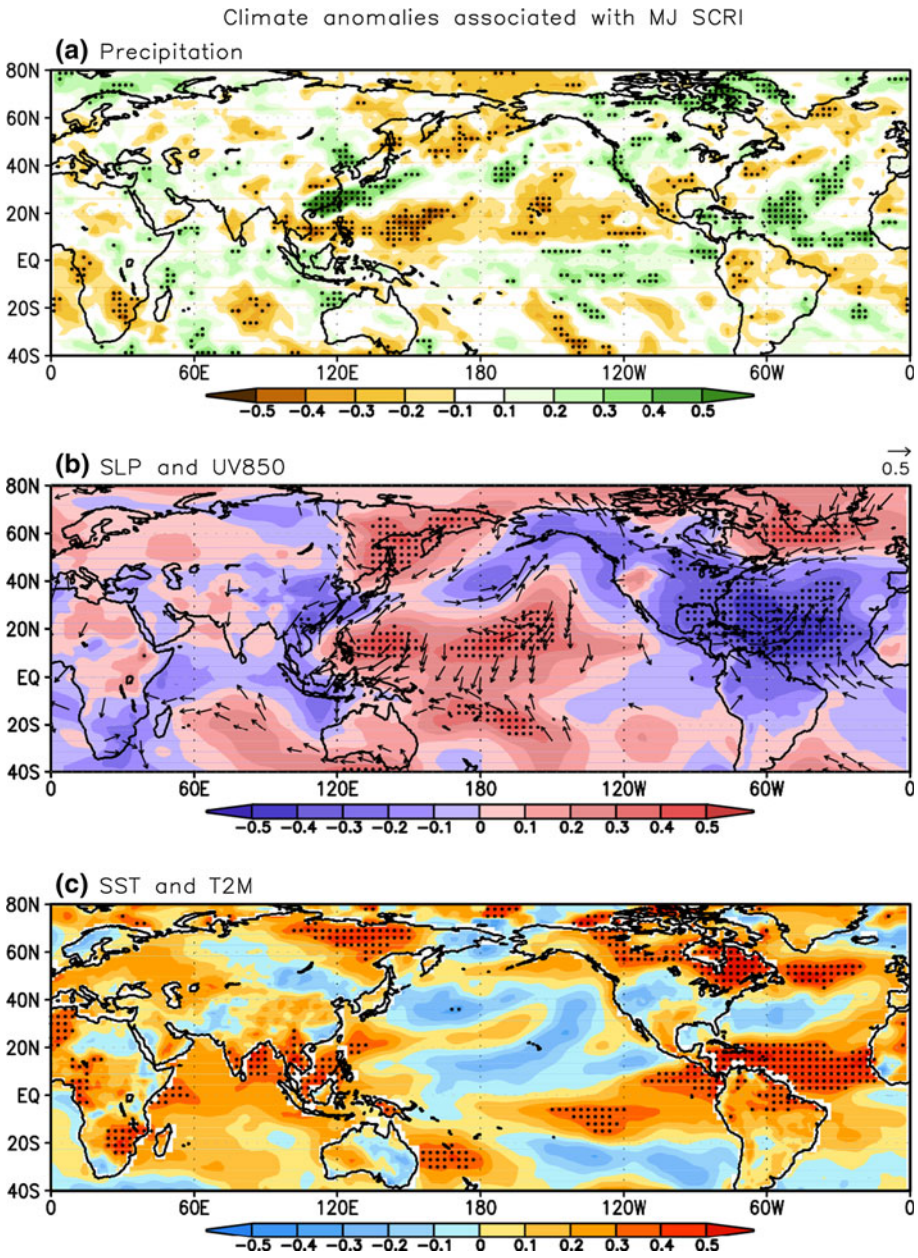

Fig. 3 Climate anomalies associated with a South China rainfall index (SCRI). The simultaneous correlation coefficient of MJ **a** precipitation, **b** SLP (*shading*) and 850 hPa-wind (UV850) anomalies, and **c** SST anomalies over ocean and 2 m air temperature (T2M) anomalies over land with respect to the MJ SCRI. The areas exceeding 95 % confidence level are *dotted* for SST and T2M. The *arrows* indicate the significant correlation at 90 % confidence level. The SCRI derived from the rain gauges stations data was used

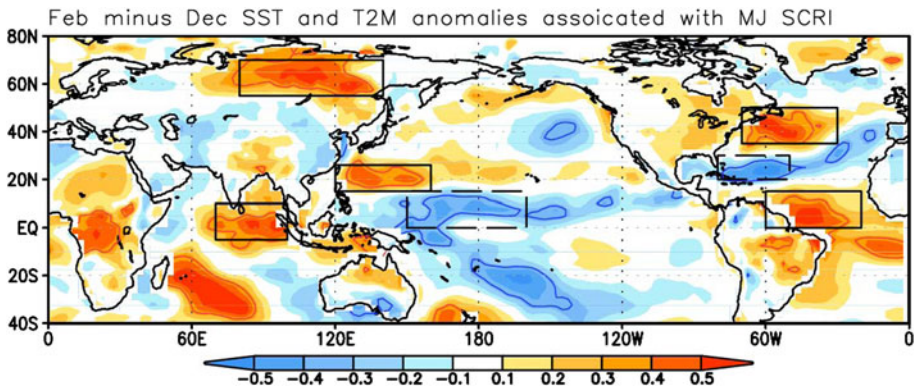

Fig. 4 Predictors for MJ South China precipitation showed by the correlation coefficient map of the tendency (Feb minus Dec) of SST over ocean and 2 m air temperature (T2M) over land with respect to the MJ SCRI. The *boxes* indicate the areas where the area-averaged variables are selected for the predictors. The *contour* indicates significance at 95 % confidence level

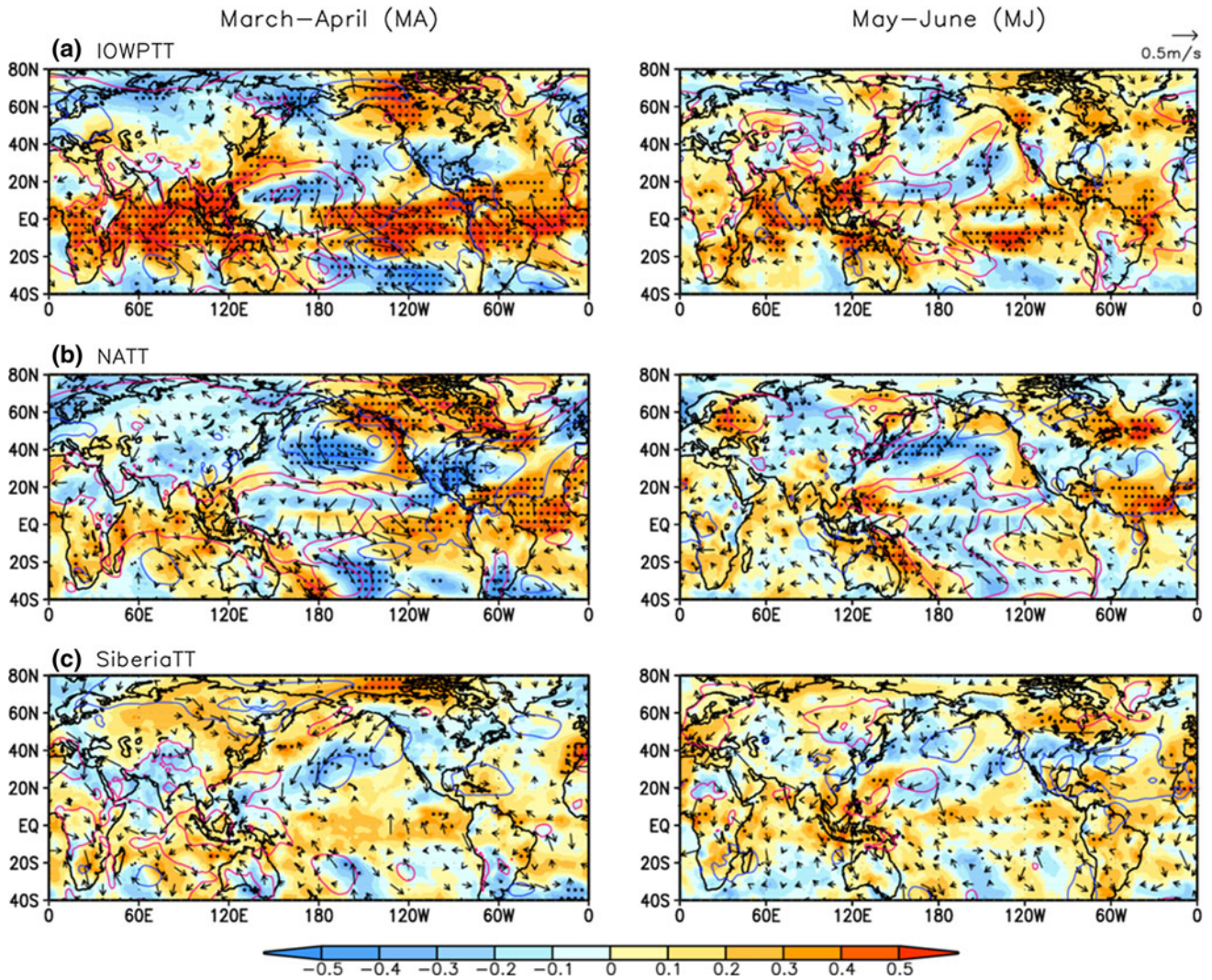

Fig. 5 March–April (MA) mean and May–June (MJ) mean T2M, SLP, and 850hP wind anomalies vectors with respect to the time series of predictors: **a** IOWPTT, **b** NATT, and **c** SiberiaTT. For T2M, the areas exceeding 95 % confidence level are *dotted*. Shown wind vectors are significant at 99 % confidence level

exciting stationary Rossby wave trains propagating from Barents Sea through Eurasian continent to EA (Ogi et al. 2004; Wu et al. 2009).

The third predictor is a winter warming process over Siberia (SiberiaTT), which might be coupled with decreasing tendency of snowfall (Ogi et al. 2004), leading to March–April warming in the eastern Siberia and further facilitate warming downstream over the Sea of Okhotsk (Fig. 5c). The warming there will enhance the barotropic blocking high over the Okhotsk Sea.

In the physical linkage between each predictor and MJ anomalies responsible for SC rainfall variability, the signals associated with all predictors tend to persist and slowly evolve from MA to MJ (Fig. 5). The interesting feature is that MJ anomalies associated with IOWPTT (Fig. 5a) look very similar to those correlated with a strong SCRI (Fig. 3c). Both the IOWPTT and NATT lead to enhanced western Pacific high pressure anomalies in MA that persist into MJ, favoring increase of the SC rainfall. Note also that the NATT signals are a generation of a wave train from North Atlantic via Eurasia to the Okhotsk Sea during MJ season, which strengthens Okhotsk High (Fig. 5b). The SiberiaTT foreshadows north Asian warming in MA and formation of the anomalous Okhotsk High in MJ.

We pointed out that the spring North Atlantic tripolar SST and Siberia surface temperature anomalies may affect an Okhotsk High. We have constructed an Okhotsk High index (OHI), which is May–June (MJ) SLP anomalies averaged over the region (45°N–65°N, 120°E−150°E). The OHI is significantly correlated with MJ SC rainfall ($r = 0.34$ at 95 % confidence level), which supports our

Table 1 Definition of each of 2-month lead predictors selected for the prediction of Southern China MJ precipitation variability

Name	Meaning	Definition
IOWPTT	February-minus-December Indo-Pacific warm pool dipolar SST	DSST (5°S–10°N, 70°E–100°E) + DSST (15°N–25°N, 120°E–160°E) − DSST (0–15°N, 150°E–160°W)
NATT	February-minus-December North Atlantic tripolar SST	DSST (0–15°N, 60°W–20°W) + DSST (35°N–50°N, 70°W–30°W) − DSST (20°N–30°N, 80°W–50°W)
SiberiaTT	February-minus-December Siberia T2M	DT2M (55°N–70°N, 80°E−140°E)

DSST (DT2M) denotes SST (2 m air temperature) tendency

Table 2 The correlation coefficients (CC) with the predictand (SCRI) and among the predictors for the period 1979–2012

	SCRI	IOWPTT	NATT	SiberiaTT
SCRI	1.0	**0.59**	**0.57**	**0.48**
IOWPTT		1.0	0.30	−0.05
NATT			1.0	0.33
SiberiaTT				1.0

The bolded numbers represent significance at 99 % confidence level. The GPCP V2, ERSST v3 data, and ERA interim data were used

arguments that an Okhotsk High can enhance SC rainfall. Furthermore, we have examined how an Okhotsk High is related to two predictors of NATT and SiberiaTT. The NATT is significantly correlated with an OHI (r = 0.43 at 99 % confidence level). The correlation coefficient between SiberiaTT and an OHI is 0.22, which indicates that SiberiaTT in the preceding winter may contribute partly to formation of anomalous Okhotsk High in MJ. The central SiberiaTT in the preceding winter tends to persist through MA into MJ and this surface warming may enhance the Lake of Baikal ridge in the mid-troposphere and could enhance the Okhotsk High.

4 A physical-empirical prediction model of South China MJ precipitation

The three predictors we found can be used for study the prediction of the MJ SC rainfall. To estimate the SC rainfall prediction, we developed a physical-empirical prediction model with stepwise multiple regression method using the predictors shown in Fig. 4. The precise definitions of the winter predictors are presented in Table 1 and their correlation coefficients with the SCRI and among the predictors are summarized in Table 2. All three predictors are selected by stepwise regression given the *F* test at 95 % confidence level. The prediction (simulation) equation is

$$\mathrm{SCRI} = 0.503 \times \mathrm{IOWPTT} + 0.382 \times \mathrm{SiberiaTT} + 0.301 \times \mathrm{NATT} \quad (1)$$

where the meaning of the predictor symbols are referred to Table 1.

Figure 6 shows the validated TCC skill for the prediction using Eq. (1). The physical-empirical model can reproduce the MJ SC rainfall realistically with a TCC skill of 0.80 for all 34 years. In addition, in order to test the predictive capability of the empirical model at the SC, the cross-validation method is performed using taking out 3 years each step. The TCC for the 34-year cross-validated reforecast skill is 0.75. To confirm whether the suggested methodology is actually useful, we used 1979–2005 data as training period to derive a prediction equation, and then

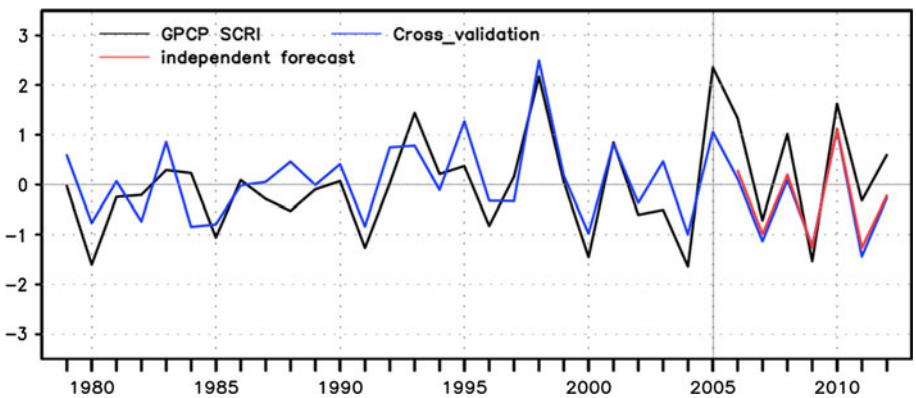

Fig. 6 Prediction skill for the physical-empirical prediction shown by the time series of observation (*black*) and cross-validated predictions by using three 2-month lead predictors (*blue*) using 34 years. The cross validation was done by taking 3-year out around the predicted year. The cross-validated correlation skill is 0.75. The 2006–2012 values (*red*) are independent test predictions, which have forecast temporal correlation skill of 0.93 when the model is built using the data in the training period of 1979–2005

made independent forecasts for the period 2006–2012. The independent forecast TCC skill of 0.93. Thus, this physical-empirical can be used to make real time forecast test.

What is the current status of the state-of-the-art climate models' prediction of the MJ SC precipitation with a 2-month lead? Figure 2b shows the performance of SC MJ rainfall prediction of current models obtained from the MME of 4 coupled models with March 1st initial condition. The TCC skill of the MME hindcast is only 0.15 for 1979–2010 period, which is much lower than the physical-empirical model prediction.

5 Concluding remarks and discussion

The South China rainfall index (SCRI) proposed here is a meaningful measure of the EA subtropical front rainfall because the SC rainfall has large coherent uniform variability and represents the maximum rainfall variability over the East Asia during early summer (MJ) (Fig. 2a). In addition, the MJ SCRI represents very well the leading EOF mode of the MJ precipitation variability over EA (Fig. 2b). Our study has for the first time attempted to explore the sources for the MJ rainfall prediction in SC.

Three physical precursors in the preceding winter have been identified. The first precursor is the development of a dipolar SST anomaly tendency in the Indo-Pacific warm pool (IOWPTT) which signifies development of Philippine Sea anomalous anticyclone that can maintain itself until early summer through anticyclone-SST dipole interaction. In addition, the warming tendency in the northern Indian Ocean which also leads to persistent SST warm anomaly over the northern Indian Ocean in ensuing spring that can enhance the Philippine Sea subtropical high during ensuing early summer. The second precursor is a tripolar SST anomaly tendency over North Atlantic (NATT), which interacts with the atmosphere and leads to a persistent tripolar North Atlantic SST anomaly pattern in MJ that can excite a teleconnection pattern to enhance the Okhotsk High, favoring enhanced rainfall in South China during early summer. The third predictor is the Siberia land warming tendency (SiberiaTT) across the winter, which might be coupled with decreasing land surface snow and it can generate local and downstream warming over the Sea of Okhotsk, contributing to increased SC rainfall.

We established a physical empirical prediction model by using these three physical meaningful predictors. The cross-validated forecast skill for the 1979–2012 period reaches 0.75. This relatively high skill provides an estimation of the lower bound for the MJ South China rainfall prediction for this period. The current dynamical models' ensemble forecast shows a low skill of 0.15 for the hindcast period of 1979–2010. Thus, our result suggests that low prediction skill of current dynamical models is largely due to models' deficiency and dynamical prediction has large room to improve.

One might wonder why ENSO did not provide a predictor. To examine whether MJ SC rainfall variability is associated with ENSO or not, the evolution of SST anomalies averaged 5°S–5°N associated with a strong SCRI were investigated from the preceding winter to the following winter (not shown). There is no significant El Nino signal in the preceding winter although a weak warming in the eastern equatorial Pacific appears during spring while dipolar SST anomaly in the Indo-Pacific warm pool region is much obvious in the preceding winter. Thus, the SCRI is much highly correlated with IOWPTT ($r = 0.59$) rather than January–February (JF) mean Nino3 SST anomaly averaged over the region (5°S–5°N, 150°W–90°W) ($r = 0.27$).

The previous studies (Kwon et al. 2007; Yim et al. 2008; Wang et al. 2009a) showed that a notable sudden change over EA around 1993–1994, which is reflected in the SC precipitation variability (Fig. 2b). If one removes the decadal signal of the MJ precipitation anomalies first, and then simulated the interannual variation using the predictors detected from interannual variation, the results are very similar to those derived with the total anomaly fields (not shown), suggesting that the predictors we have selected from the total anomalies might have included interdecadal variation signals.

Here we focus on early summer (MJ). To some extent this division of summer season is for convenience of practical use. More accurate division may be achieved by using natural sudden change (singularity) points in the seasonal cycle. There are significant monsoon singularities in the EA and western North Pacific (WNP) region (Wang and Xu 1997). The South China Sea monsoon onset in mid-May and the termination of Meiyu/Baiu in mid-July are salient seasonal singularities during which the atmospheric circulation experiences drastic changes (LinHo 2002). One could divide May10th–July 10th as early summer. However, the difference is expected to be small compared to MJ, while use of MJ is more convenient for issuing climate forecast to public.

Acknowledgments This work was supported from Asian-Pacific Economic Cooperation (APEC) Climate Center, the National Research Foundation of Korea (NRF) through a Global Research Laboratory (GRL) grant (MEST 2011-0021927), and IPRC, which is in part supported by JAMSTEC, NOAA, and NASA. This is the SOEST publication number 9048 and IPRC publication number 1029.

References

Dee DP et al (2011) The ERA-interim reanalysis: configuration and performance of the data assimilation system. Q J R Meteorol Soc 137:553–597

Delworth TL, Broccoli AJ, Rosati A et al (2006) GFDL's CM2 global coupled climate models. Part I: formulation and simulation characteristics. J Clim 19:643–674

Ding YH (1992) Summer monsoon rainfalls in China. J Meteor Soc Japan 70:373–396

Hudson D, Alves O, Hendon HH, Wang G (2011) The impact of atmospheric initialisation on seasonal prediction of tropical Pacific SST. Clim Dyn 36:1155–1171

Huffman GJ, Bolvin DT, Adler RF (2011) Last updated GPCP Version 2.2 combined precipitation data set. WDC-A, NCDC, Asheville, NC (2011). Dataset accessed at http://www.ncdc.noaa.gov/oa/wmo/wdcamet-ncdc.html

Kwon M, Jhun JG, Ha KJ (2007) Decadal change in east Asian summer monsoon circulation in the mid-1990s. Geophys Res Lett 34:L21706. doi:10.1029/2007GL031977

Lau NC, Leetmaa A, Nath MJ, Wang HL (2005) Influences of ENSO-induced Indo–western Pacific SST anomalies on extratropical atmospheric variability during the boreal summer. J Clim 18:2922–2942

LinHo Wang B (2002) The time-space structure of the Asian-Pacific summer monsoon: a fast annual cycle view. J Clim 15: 2001–2019

Luo JJ, Masson S, Behera S, Shingu S, Yamagata T (2005) Seasonal climate predictability in a coupled OAGCM using a different approach for ensemble forecast. J Clim 18:4474–4497

Ogi M, Tachibana Y, Yamazaki K (2004) The connectivity of the winter North Atlantic Oscillation (NAO) and the summer Okhotsk High. J Meteor Soc Japan 82:905–913

Panofsky HA, Brier GW (1968) Some applications of statistics to meteorology. Pennsylvania State University Press, University Park, PA, p 224

Qin S, Riyu L, Chaofan L (2013) Large-scale circulation anomalies associated with interannual variation in monthly rainfall over South China from May to August. Adv Atmos Sci. doi:10.1007/s00376-013-3051-x

Saha S et al (2013) The NCEP climate forecast system version 2. J Clim (accepted)

Smith TM, Reynolds RW, Peterson TC, Lawrimore J (2008) Improvements to NOAA's historical merged land-ocean surface temperature analysis (1880–2006). J Clim 21:2283–2296

Tao S, Chen L (1987) A review of recent research on the East Asia summer monsoon in China. In: Chang C-P, Krishnamurti TN (eds) Monsoon Meteorology. Clarendon Press, pp 60–92

Wang B, Xu X (1997) Northern Hemisphere summer monsoon singularities and climatological intraseasonal oscillation. J Clim 10:1071–1085

Wang B, Wu R, Fu X (2000) Pacific-East Asia teleconnection: how does ENSO affect East Asian climate? J Clim 13:1517–1536

Wang B, Liu J, Yang J, Zhou T, Wu Z (2009a) Distinct principal modes of early and late summer rainfall anomalies in East Asia. J Clim 22:3864–3875

Wang B, Lee JY et al (2009b) Advance and prospectus of seasonal prediction: assessment of the APCC/CliPAS 14-model ensemble retroperspective seasonal prediction (1980–2004). Clim Dyn 33:93–117

Wang B, Liu J, Kim HJ, Webster P, Yim SY (2012) Recent change of the global monsoon precipitation (1979–2008). Clim Dyn 39:1123–1135. doi:10.1007/s00382-011-1266-z

Wang B, Xiang B, Lee JY (2013) Subtropical high predictability establishes a promising way for monsoon and tropical storm predictions. PNAS 10:2718–2722

Wu R, Wang B (2002) A contrast of the East Asian summer monsoon and ENSO relationship between 1962–1977 and 1978–1993. J Clim 15:3266–3279

Wu Z, Wang B, Li J, Jin FF (2009) An empirical seasonal prediction of the east Asian summer monsoon using ENSO and NAO. J Geophys Res 114:D18120. doi:10.1029/2009JD011733

Xiang B, Wang B (2013) Mechanisms for the advanced Asian summer monsoon onset since the mid-to-late 1990 s. J Clim. doi:10.1175/JCLI-D-12-00445.1

Yim SY, Jhun JG, Yeh SW (2008) Decadal change in the relationship between east Asian-western North Pacific summer monsoon and ENSO in the mid-1990 s. Geophys Res Lett 35:L20711. doi:10.1029/2008GL035751

Yun KS, Seo KH, Ha KJ (2010) Interdecadal change in the relationship between ENSO and the intraseasonal oscillation in East Asia. J Clim 23:3599–3612

Zhou T, Yu R, Li H, Wang B (2008) Ocean forcing to changes in global monsoon precipitation over the recent half-century. J Clim 21:3833–3852

Zhou T, Gong D, Li J, Li B (2009) Detecting and understanding the multi-decadal variability of the East Asian Summer Monsoon—recent progress and state of affairs. Meteorol Z 18:455–467